JOURNAL OF
Bioactive
and
Compatible
Polymers

Original Article

Journal of Bioactive and
Compatible Polymers
2016, Vol. 31(5) 453–466

DOI: 10.1177/0883911516631354
jbc.sagepub.com
SAGE

Potential of mannan or dextrin nanogels as vaccine carrier/adjuvant systems

Catarina Gonçalves[1*], Sílvia A Ferreira[1*], Alexandra L Correia[2], Célia Lopes[2,3], Carolina E Fleming[2,3], Eduardo Rocha[2,3], Manuel Vilanova[2,4] and Miguel Gama[1]

Abstract

Polymeric nanogels have been sophisticatedly designed promising a new generation of vaccine delivery/adjuvant systems capable of boosting immune response, a strategic priority in vaccine design. Here, nanogels made of mannan or dextrin were evaluated for their potential as carriers/adjuvants in vaccine formulations. Since lymph nodes are preferential target organs for vaccine delivery systems, nanogels were biotin-labeled, injected in the footpad of rats, and their presence in draining lymph nodes was assessed by immunofluorescence. Nanogels were detected in the popliteal and inguinal lymph nodes by 24 h upon subcutaneous administration, indicating entrapment in lymphatic organs. Moreover, the model antigen ovalbumin was physically encapsulated within nanogels and physicochemically characterized concerning size, zeta potential, ovalbumin loading, and entrapment efficiency. The immunogenicity of these formulations was assessed in mice intradermally immunized with ovalbumin–mannan or ovalbumin–dextrin by determining ovalbumin-specific antibody serum titers. Intradermal vaccination using ovalbumin–mannan elicited a humoral immune response in which ovalbumin-specific IgG1 levels were significantly higher than those obtained with ovalbumin alone, indicating a T_H2-type response. In contrast, dextrin nanogel did not show adjuvant potential. Altogether, these results indicate that mannan nanogel is a material that should be explored as a future antigen delivery system.

Keywords

Mannan, dextrin, nanogels, lymph node, ovalbumin, vaccination

*Catarina Gonçalves (cgoncalves@deb.uminho.pt) and Sílvia A Ferreira (silviarmferreira@gmail.com) contributed equally to this work.

[1]Centro de Engenharia Biológica, Universidade do Minho, Braga, Portugal
[2]Instituto de Ciências Biomédicas de Abel Salazar, Universidade do Porto, Porto, Portugal
[3]Centro Interdisciplinar de Investigação Marinha e Ambiental, Universidade do Porto, Porto, Portugal
[4]Instituto de Biologia Molecular e Celular, Universidade do Porto, Porto, Portugal

Corresponding author:
Miguel Gama, Centro de Engenharia Biológica, Universidade do Minho, Campus de Gualtar, 4710-057 Braga, Portugal.
Email: fmgama@deb.uminho.pt

Introduction

Nanotechnology plays a significant role in vaccine development and has emerged as a new approach in the design of vaccines. Different polymers have been synthesized or modified for biomedical applications.[1,2] Polysaccharides have been used to synthesize nanogels; these are nano-sized hydrophilic three-dimensional macromolecular networks. The properties of nanogels, such as flexible mesh, high water content, and high loading capacity, permit the carrying of antigens.[3,4] Nanogels are expected to overcome vaccination hurdles, such as inadequate antigen biodistribution, short half-life, and limited bioavailability upon administration while also protecting the associated antigen from adverse physiologic conditions, such as enzyme degradation and/or physical alteration such as aggregation or precipitation.[5] An increased interaction between immune cells and antigens has been observed when antigens are coupled to nanogels. This increased interaction modulates and improves the antigen-specific immune response and is known as the adjuvant effect. Antigen-presenting cells (APCs) such as dendritic cells and macrophages are fundamental in initiating and modulating the immune response as they capture, process, and present the antigen to T cells.[6] T cells may also have adjuvant activity to B cells, measured by assessing the levels and isotypic profile of immunoglobulin (Ig)G levels in a secondary immune response. A classic example can be the predominant production of IgG2a and IgG1 isotypes, associated with T_H1- and T_H2-type immune responses in the murine host, respectively.[7] Most adjuvants provide danger signals to help elicit an immune response against vaccine antigens. The usage of a nano-particulate antigen delivery system may help target the antigen to specialized APCs; there should be no adverse effect of the carrier alone.[8] When administered intramuscularly or subcutaneously, vaccines are drained into regional lymph nodes, where T and B cells may encounter their cognate antigen and cooperatively mount a specific immune response and generate memory cells.[9] For pathogens such as extracellular bacteria or viruses, an effective vaccine usually induces a strong neutralizing antibody response.[10] Therefore, the formulation should reach the lymph nodes and establish the appropriate cell interactions in order to achieve effective and durable immunity. This formulation should avoid using organic solvents and high temperatures so as to preserve the antigenic epitopes.[11–13]

Although the encapsulation of antigens into polymeric vaccines has been explored, few strategies are currently undergoing clinical evaluation.[14] The properties of tunable nanocarriers—including material chemistry, size, and shape; surface charge; and hydrophobicity/hydrophilicity—impact nanocarrier success in preventive or therapeutic vaccination.[3,15,16]

Previously, we reported the production and characterization of mannan- or dextrin-based nanogels. Polymers are natural, medical grade, and biocompatible. The respective nanogels are obtained through a simple methodology and moderate conditions. Despite the mentioned advantages, mannan- or dextrin-based nanogels have never been explored for vaccination purposes. Briefly, the hydrophilic natural polymers are modified grafting long alkyl chains to promote self-assembly of the amphiphilic polymer in water, leading to the nanogel formation.[17,18] Nanogel loading with proteins and their release were also reported.[19] The internalization of mannan or dextrin nanogels in vitro by macrophages[20,21] and their ability to carry biologically active agents[22,23] led us to explore their potential as vaccine delivery/adjuvant systems, using ovalbumin (OVA) as a model antigen.[24,25] In addition, mannan potentially targets APCs since dendritic cells and macrophages express on their surface mannose receptors, which recognizes carbohydrates present on the cell walls of infectious agents.

In this work, OVA-nanogel formulations were characterized by size, surface charge, OVA loading and entrapment efficiency. The presence of nanogels in proximal lymph nodes (popliteal and inguinal) after subcutaneous administration was evaluated by immunofluorescence and complement system activation was assessed by western blot. The extent and type of immune response

elicited after intradermal administration of the OVA-nanogel formulations were evaluated in mice by assessing the production of OVA-specific antibodies and their isotypic profile.

Materials and methods

Materials

Cobra venom factor was purchased from Quidel Corporation (USA), mouse monoclonal antibody specific for human C3 from Abcam (UK) and the secondary polyclonal goat anti-mouse IgG antibody conjugated with alkaline phosphatase from Dako (Denmark). 5-Bromo-4-chloro-3-indolyl phosphate (BCIP), *O*-(2-aminoethyl)-*O′*-[2-(biotinylamino)ethyl]octaethylene glycol, sodium borohydride, bovine serum albumin (BSA), apyrogenic phosphate buffered saline (PBS), 4-nitrophenylphosphate disodium salt hexahydrate and the limulus amebocyte lysate test (E-toxate™) were obtained from Sigma (USA). Ketamine (Imalgéne 1000) and xilazine (Rompum) were acquired from Bayer (Portugal). Optimal cutting temperature (OCT) compound and streptavidin dylight 488 were purchased from Thermo Fisher Scientific (USA) and 2-methyl butane from VWR International (France). Goat normal serum (Histostain Plus Blocking Solution) and Alexa Fluor® 568 goat anti-mouse IgG were obtained from Invitrogen, Life Technologies (USA). The primary antibody mouse anti-rat CD169 (clone ED3) was purchased from Serotec (USA) and 4′,6-diamidino-2-phenylindole (DAPI) containing mounting media (Vectashield H200; Vector, USA). Polymyxin B column and bicinchoninic acid (BCA) protein assay were purchased from Pierce (USA), Microcon® Centrifugal Filter Devices, with 100,000 nominal molecular weight (Mw), from Millipore (Darmstadt, Germany), Minisart® syringe filters (pore size 0.22 μm) from Sartorius Stedim Biotech (Germany) and the molecular-weight protein ladder standard (PageRuler Prestained Protein Ladder) from Fermentas (USA). The antibodies goat anti-mouse IgM, IgG1, IgG2a, IgG3, and IgA conjugated to alkaline phosphatase human adsorbed were purchased from Southern Biotech (USA).

Mannan–vinyl methacrylate (VMA)-SC_{16}[22] and dextrin–vinyl acrylate (VA)-SC_{16}[18] were synthesized as comprehensively described before. Mannan–VMA-SC_{16} is composed by the hydrophilic mannan (Mw 85,000) backbone with grafted vinyl methacrylate (VMA) ester groups, which are partially substituted with long alkyl (hydrophobic) chains (SC_{16}) via Michael addition. Dextrin–VA-SC_{16} is composed by the hydrophilic dextrin (Mw 2000) backbone with grafted vinyl acrylate (VA) ester groups, which are also partially substituted with SC_{16} chains. In this work, the following nanogels were used: (1) mannan–VMA-SC_{16} with degrees of substitution per 100 mannose residues of 31 and 20, respectively, for the acrylate groups (DS_{VMA} 31%) and alkyl chains (DS_{C16} 20%) and (2) dextrin–VA-SC_{16} with degree of substitution per 100 dextrin glucopyranoside residues of 30 and 5, respectively, for the acrylate groups (DS_{VA} 30%) and alkyl chains (DS_{C16} 5%). The sterile colloidal dispersion stocks of nanogel were prepared by stirring the lyophilized modified polymer (mannan or dextrin) in sterile apyrogenic PBS, pH 7.4, followed by sterilizing filtration with Minisart syringe filters (pore size 0.22 μm). The nanogel formation was confirmed by dynamic light scattering (DLS).

Complement activation assay

To determine whether nanogels activated the complement cascade, the protocol described by the Nanotechnology Characterization Laboratory for qualitative determination of total complement activation by Western blot analysis[19] was performed. Briefly, equal volumes (50 μL) of human plasma from healthy donors, veronal buffer, and sample—mannan or dextrin nanogel colloidal

dispersion in PBS (1.0 mg/mL), cobra venom factor as positive control, or PBS as negative control—were mixed together and incubated for 1 h at 37°C. Proteins were resolved using 10% sodium dodecyl sulphate–polyacrylamide gel electrophoresis (SDS-PAGE), and then transferred to a Immun-Blot PVDF membrane using the Trans-Blot® SD semidry transfer equipment (Bio-Rad, USA). The membranes were incubated for 90 min with a mouse monoclonal antibody specific for human C3 diluted 1:1000 followed by washes and incubation with secondary polyclonal goat anti-mouse IgG antibody conjugated with alkaline phosphatase diluted 1:2000. The membrane was finally revealed with BCIP. The C3 cleavage was evaluated by densitometry using image analysis software (NIH Image J software, U. S. National Institutes of Health, Bethesda, Maryland, USA).

Biotin-labeled nanogels

The strategy used, in this work, for the conjugation of biotin to nanogels is the covalent binding through a conjugate addition reaction (1,4 addition) between the acrylate-functionalized polymer (dextrin or mannan) and biotin. The biotin acts as nucleophile added to the β-carbon of the α, β-unsaturated carbonyl present in acrylate-functionalized polymer.

In order to label nanogels with biotin, the following solutions were prepared: (1) nanogel solution—10.0 mg of either mannan–VMA-SC_{16} or dextrin–VA-SC_{16} dissolved in 4.0 mL of sterile apyrogenic water and (2) biotin solution—6.0 mg of *O*-(2-aminoethyl)-*O′*-[2-(biotinylamino) ethyl]octaethylene glycol dissolved in 2.0 mL of sterile apyrogenic water. These two solutions were mixed up and stirred for 72 h at 50°C. Unbound biotin was separated by dialysis using regenerated cellulose tubular membranes, with a 1000 nominal molecular weight cut off (OrDial D-Clean, Orange Scientific, Belgium) against water for 48 h, with frequent water changes. After freezing, the mixture was lyophilized and stored. Biotinylation was confirmed by the reduction in signal assigned to acrylate groups upon Proton nuclear magnetic resonance (^{1}H-NMR) analysis, due to biotin linkage. Otherwise, biotinylation did not affect the nanogel size distribution, as evaluated by DLS.

Lymph node drainage: immunofluorescence study

Wistar rats were chosen in this study, to avoid difficulties in the collection of the very small lymph nodes in mice—the model used in the immunization studies. Twelve Wistar rats (males, 15-week old, 320–340 g) were purchased from Charles River (Barcelona, Spain). The animals, kept at the animal facilities of the Instituto de Ciências Biomédicas de Abel Salazar (ICBAS), Universidade do Porto (U.Porto), Portugal, during the experiments, were divided into two groups (six rats in each one) and anesthetized with intraperitoneal injection of ketamine (100 mg/kg) and xilazine (10 mg/kg). The rats were injected into the footpad (right side) with 100 μL of biotin-labeled dextrin or mannan nanogel (1.0 mg/mL in sterile apyrogenic PBS). The left-side footpad was thus used as negative control. Twenty-four hours after injection, the rats were euthanized by decapitation. Popliteal and inguinal lymph nodes were collected and embedded in OCT compound, frozen in 2-methyl butane cooled in liquid nitrogen and stored in a −80°C freezer. Cryosections (4 μm) were obtained in a cryostat (Leica CM1850), attached to silane-coated slides, air dried, and stored at −80°C before staining.

Cryosections were fixed in cold (−20°C) acetone for 2 min, then in freshly prepared paraformaldehyde/lysine/periodate (PLP) fixative for 8 min and finally further treated with 0.1% sodium borohydride in PBS—to quench autofluorescence. Nonspecific binding was blocked with 10% BSA in PBS for 20 min and goat normal serum for an additional 20 min. For macrophage immunostaining, cryosections were incubated overnight at 4°C with the mouse anti-rat CD169 (a cell

surface antigen expressed predominantly by macrophages confined to lymphoid organs only) primary antibody (clone ED3), diluted at 1:50 in PBS with 5% BSA. Then after, Alexa Fluor 568 goat anti-mouse IgG diluted at 1:500 in PBS with 5% BSA was applied for 1 h, at room temperature. Biotin-labeled nanogels were stained for 1 h with Streptavidin Dylight 488, diluted 1:200 in PBS with 5% BSA, at room temperature. Slides were carefully rinsed with 0.01 M PBS, pH 7.5, after all incubations. Finally, slides were counterstained with DAPI containing mounting media Vectashield H200, coverslipped, and sealed with nail polish. Cryosections were visualized and photographed using an inverted fluorescent microscope (Olympus IX7) coupled with a cooled digital color camera (Olympus DP71).

Preparation and characterization of OVA-nanogel formulations

OVA (Grade III, Mw 45 kDa; Sigma) solutions in PBS were depleted of contaminating endotoxin using a polymyxin B column and tested by the limulus amebocyte lysate test (E-toxate™). All OVA formulations used in this study tested endotoxin free.

The OVA (0.2 mg/mL) incorporation within nanogels (4.0 mg/mL) in PBS, after 24 h of incubation at 25°C, was evaluated using an ultrafiltration method—5 min at 10,000*g* to collect the filtrate—using Microcon (100,000) Centrifugal Filter device. The retentate was washed twice with PBS. Initial sample and all collected filtrate and retentate samples had a fixed final volume adjusted with PBS. Empty nanogel colloidal dispersion (4.0 mg/mL) and OVA solution (0.2 mg/mL) in PBS were used as controls and subjected to the same procedure. The OVA association with nanogel was evaluated by analyzing initial sample, filtrate and retentate fractions by SDS-PAGE and BCA protein assay. Each sample (10 μL) was diluted with PBS (10 μL) and proteins were desorbed from the nanogel by adding SDS loading buffer (4 μL) followed by 6–10 min of boiling. Samples were resolved using 12% or 15% SDS-PAGE, for mannan or dextrin formulations, respectively. Each gel run included one lane of a Mw protein ladder standard. Gels were silver-stained. For all samples, the OVA concentration was determined with BCA protein assay following the manufacturer's instructions. Each sample was assessed in triplicate and the absorbance of the nanogel fractionated samples was subtracted from those of the OVA-loaded counterparts. The results were expressed as the weight ratio of protein per nanogel (μg/mg). Besides, the loading efficiency was defined as the percentage of OVA loaded relating to the initial amount of protein.

Mice immunization

Male BALB/c mice (15-week old) were purchased from Charles River (Barcelona, Spain). Animals were kept at the animal facilities of the ICBAS—U.Porto during the experiments. Hiding and nesting materials were provided as enrichment. Procedures involving mice were performed according to the European Convention for the Protection of Vertebrate Animals used for Experimental and Other Scientific Purposes (ETS 123) and 86/609/EEC Directive and Portuguese rules (DL 129/92).

Mice were trice-immunized intradermally (prime, first boost and second boost) with 20 μg of OVA formulated with one of the following delivery vehicles (100 μL): PBS, mannan, or dextrin nanogel (400 μg) in PBS incorporated for 24 h at 25°C. Two additional control groups were used, mannan or dextrin (400 μg/100 μL) nanogels in PBS.

Boost immunizations were done 13 and 24 days after priming. Blood samples were collected 13 days after priming, 11 days after first boost and 28 days after second boost, allowed to clot overnight at 4°C to prepare serum sample aliquots that were stored at −20°C until used for antibody detection.

Titration of OVA-specific antibody in serum

OVA-specific IgM, IgG1, IgG2a, IgG3 and IgA antibodies were quantified in serum samples by enzyme-linked immunosorbent assay (ELISA). In brief, microtiter flat-bottom 96-well plate was coated overnight at 4°C with 5 μg/mL OVA solution in PBS (50 μL per well). After washing with TST buffer [Tris-buffered saline (10 mM Tris base, 150 mM NaCl), pH 8.0, containing 0.05% Tween 20], blocking solution, TST buffer with 2% BSA, was added (200 μL per well) and incubated for 1 h at room temperature. After discarding the block solution, serial dilutions of the serum samples in TST with 1% BSA were then plated (50 μL per well) and incubated for 1 h at room temperature. After washing with TST buffer, the secondary antibody goat anti-mouse IgM, IgG1, IgG2a, IgG3, and IgA conjugated to alkaline phosphatase human adsorbed diluted 1:500 was incubated 1 h at room temperature (50 μL per well). After washing with TST buffer, the bound antibodies were detected by development at room temperature, protected from light, using a substrate solution (50 μL per well) of 4-nitrophenylphosphate disodium salt hexahydrate dispersed in 5 mL of alkaline phosphatase buffer (50 mM Na_2CO_3, 1 mM $MgCl_2$), pH 9.8. The reaction was stopped by the addition of 0.1 M ethylenediaminetetraacetic acid (EDTA), pH 8.0 (50 μL per well). The absorbance was measured at 405 and at 570 nm as reference with a spectrophotometer (Original Multiskan Ex; Thermo Electron Corporation, Waltham, MA, USA). The antibody titers were expressed as the reciprocal of the highest dilution giving an absorbance of 0.1 above that of the control (no serum added).

Statistical analysis

The results were expressed as mean ± standard deviation (SD) for each group and statistical analysis was carried out using one-way analysis of variance (ANOVA) with Bonferroni's multiple comparison post-test using GraphPad Prism version 4.00 for Windows (GraphPad Software, La Jolla, CA, USA).

Results and discussions

Nanogels and OVA-nanogel formulations

Nanogels are obtained by dispersion of lyophilized modified polymer in aqueous solution which is subsequently sterilized.[17,18] OVA loading is done through incubation of OVA with nanogels that are then purified. Therefore, the preparation conditions avoid the use of organic solvents, high temperatures or otherwise harsh conditions which would compromise or aggregate the antigen.

The prepared nanogels or OVA-nanogel formulations were characterized regarding their size distribution and zeta potential (Table 1).

OVA–mannan formulation presents a mean hydrodynamic diameter and a near neutral surface charge, similar to those obtained for empty mannan nanogel. OVA–dextrin formulation presents a ≈nine times lower diameter and similar zeta potential compared to OVA–mannan. The results obtained reveal that OVA incorporation within nanogels (mannan or dextrin) did not alter nanogel size or surface charge.

The size of a delivery system can influence its biodistribution and consequently the fate of the antigen in vivo. Small particles can easily penetrate the extracellular matrix and enter directly into the lymphatic vessels. Larger particles will mainly linger at the administration site as they cannot pass through the extracellular matrix.[26] The surface charge also plays a significant role in the activation of the immune response. Thiele et al.[27] showed that the uptake of polystyrene nanoparticles

Table 1. Size (diameter and polydispersity index) and zeta potential measurements obtained at 37°C for mannan or dextrin nanogels (4.0 mg/mL in PBS), OVA–mannan or OVA–dextrin formulations (OVA 0.2 mg/mL and nanogels 4.0 mg/mL in PBS).

	Mannan nanogel	OVA–mannan nanogel	Dextrin nanogel	OVA–dextrin nanogel
Diameter (nm)	240.9 ± 6.7	234.3 ± 8.5	23.3 ± 0.4	27.1 ± 1.4
Polydispersity index	0.618 ± 0.099	0.702 ± 0.022	0.495 ± 0.009	0.339 ± 0.028
Zeta potential (mV)	−9.69 ± 2.00	−10.90 ± 1.43	−9.92 ± 1.95	−10.10 ± 1.62

OVA: ovalbumin; PBS: phosphate buffered saline; SD: standard deviation.
Values represent mean ± SD ($n = 5$).

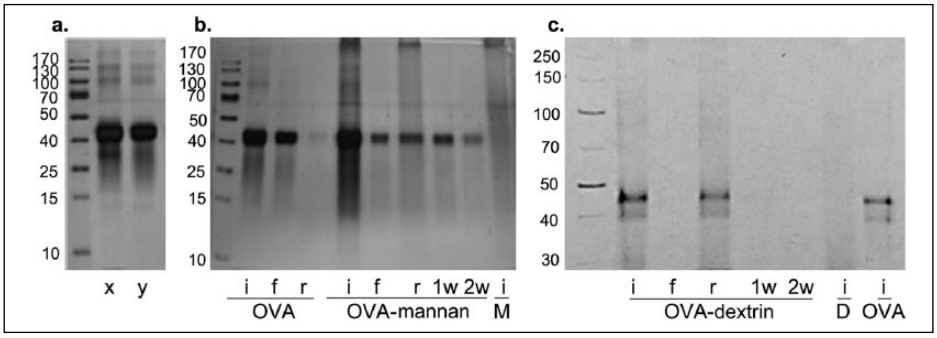

Figure 1. Silver-stained SDS-PAGE gels of (a) OVA (0.2 mg/mL) comparing the freshly prepared (x) with the one incubated 24 h at 25°C (y); (b) OVA solution (0.2 mg/mL in PBS), OVA–mannan formulations and mannan nanogel (M, 4.0 mg/mL in PBS) and (c) OVA–dextrin formulations and dextrin nanogel (D, 4.0 mg/mL in PBS). Formulations were obtained by incorporation (24 h at 25°C) of OVA (0.2 mg/mL) within nanogel dispersed in PBS (4.0 mg/mL)—initial sample (i), first filtrate (f), and retentate obtained after washing (r): first wash (1w) and second wash (2w).

by macrophages and dendritic cells can be strongly enhanced in vivo for particles bearing a cationic surface. Interestingly, when comparing the dendritic cell uptake of polystyrene spheres of 100 and 1000 nm with different surface charge, Foged et al.[28] observed that the cationic coating increased the uptake of larger particles, while smaller ones seem to undergo equal uptake independently to their surface charge.

Following loading of nanogels with OVA, samples were subjected to purification using Microcon centrifugal devices to remove free protein, allowing the determination of OVA loading and entrapment efficiency. Initial and fractionated samples were analyzed by SDS-PAGE (Figure 1). No degradation of the protein was detected after the incubation period (Figure 1(a)). As expected, free OVA flowed through the ultrafiltration device (Figure 1(b)), allowing effective removal of the non-encapsulated protein in nanogel formulations.

Entrapment efficiency can be qualitatively estimated from Figure 1. Comparing mannan (Figure 1(b)) and dextrin (Figure 1(c)) nanogels, it can be concluded dextrin allows more efficient entrapment. After centrifugation of the mannan formulation, OVA was detected in the filtrate (f) and in the first (1w) and second wash (2w). However, some protein still remained in the retentate (r). In the case of the dextrin formulation, OVA was not detected in the filtrate nor in the wash fluids. OVA was detected in the retentate (r) in amounts roughly comparable to the initially loaded protein.

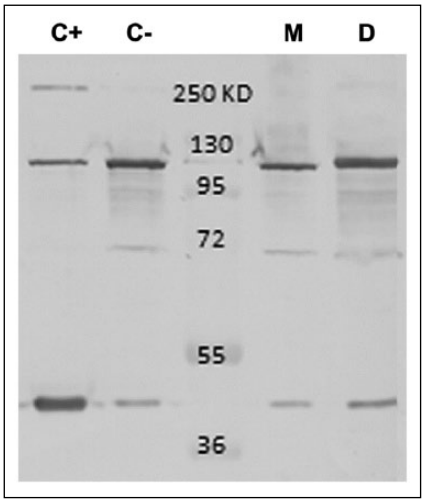

Figure 2. Analysis of complement system activation by Western blot for mannan nanogel (M) and dextrin nanogel (D). Cobra venom factor was used as positive control (C+) and PBS as negative control (C−). The upper band of ~115 kDa corresponds to C3 (α chain) and the lower band ~43 kDa corresponds to C3-cleavage product(s) (C3c, iC3b[C3α']). C3 cleavage was evaluated by densitometry using image analysis software (NIH Image J software), after normalizing the percentage of the lower band of the positive control as the maximum cleavage that can be achieved (100%): 41 ± 8% for negative control, 33 ± 7% for mannan nanogel, and 37 ± 2% for dextrin nanogel.

A BCA protein assay was performed to quantify the protein content of the retentate (after ultrafiltration), giving 16.6 ± 7.2 and 39.2 ± 4.7 OVA μg/mg for mannan and dextrin nanogels, respectively, corresponding to a loading efficiency of 36.3 ± 6.1% and 78.5 ± 9.3%, respectively. Therefore, a much higher loading efficiency was obtained for dextrin formulations.

Complement activation

Complement activation can enhance immune response by promoting chemotaxis, macrophage phagocytosis, B-cell activation through CD21 binding and antigen presentation by follicular dendritic cells.[29] However, excessive inflammation and anaphylaxis are possible serious side effects of complement activation.[30,31] Therefore, the extent of complement activation induced by nanogels was examined in an in vitro assay, using human plasma aliquots pretreated with nanogels.

As demonstrated in Figure 2, mannan or dextrin nanogels raised similar levels of C3-cleavage products as the negative control, indicating they did not induce the in vitro activation of the complement cascade. Therefore, it is unlikely they would induce a deleterious inflammatory response due to complement activation in vivo.

Nanogel capture by macrophages in lymph nodes

It is generally accepted that vaccine delivery systems (liposomes, microspheres, nanoparticles, emulsions) are recognized by APCs and promote uptake of the associated antigen.[32] However, their migration toward the lymph nodes and subsequent retention, a crucial step in immune response initiation, has not been fully explored. The lymph node is a privileged target organ for vaccine delivery providing an adequate cellular and molecular environment for the activation of B and T cells.

The pharmacokinetics of nanoparticles to lymphatics from the injection site depends on both the physiological structure of interstitial space and lymphatic system and on the nanoparticle physicochemical properties such as surface charge, size, or colloidal stability.[33] In the lymph nodes, particles can get mechanically filtered out in the reticular meshwork of the sinuses or be internalized by macrophages and/or dendritic cells. Particles not trapped by the first encountered lymph node will follow the lymph downstream to the next one.[34] One challenge in the development of effective vaccine carriers lies on obtaining efficient taken up into lymphatics, retention, and internalization by APCs. Reddy et al.[35] showed that nanoparticles smaller than 50 nm in diameter are more efficiently transported to regional draining lymph nodes, via interstitial flow, and internalized by lymph node DCs. Nanoparticles bigger than 100 nm remain near the administration site, where they may be internalized by immature peripheral dendritic cells that then migrate to lymph nodes, mature, and present antigen to T cells.[36,37]

In order to assess the presence of nanogels in the proximal lymph nodes, rats were injected in the footpad with biotin-labeled nanogels. Twenty-four hours after administration, popliteal and inguinal lymph nodes were collected. Antigens carried to the lymph nodes by the afferent lymph must pass a macrophage-rich zone that lies underneath the subcapsular sinus before reaching the B cell–rich follicles.[38] Subcapsular sinus macrophages by sampling antigens at the lymph–tissue interface may function as a first line of APCs.[33] These APCs may also display antigens able to be directly recognized by lymph node B cells.[39,40] Therefore, we assessed whether the nanogels used could also target these cells. Cryosections of lymph nodes showed the presence of nanogels in the popliteal lymph node (in green on Figure 3) within 24 h of injection.

The presence of nanogels in the inguinal lymph node was verified 24 h after subcutaneous administration.

Notably, both nanogels co-localized with macrophages ($CD169^+$), essentially underneath the subcapsular sinus; however, mannan seems to penetrate further into the lymph node than dextrin nanogels, probably reaching the B cell–rich follicles. As the presence of nanogels in both the popliteal and inguinal lymph nodes was effective for at least for 24 h, it shows an important entrapment of the nanogels in these lymphatic organs. Macrophages were shown to retain antigens for even longer periods;[41] therefore, persistence of antigens delivered in this way may be expected.

Specific antibody response in serum induced by immunization using OVA-nanogel formulations

The effect of mannan or dextrin nanogel on the magnitude of the humoral immune response in OVA-immunized mice was evaluated by assessing the serum titers of OVA-specific antibodies of isotypes IgA, IgG1, IgG2a, IgG2b, IgG3, and IgM. The OVA–mannan formulation leads to an increase in the serum levels of OVA-specific IgG1 antibodies elicited by immunization, as compared to OVA alone, indicating that mannan nanogel provided an adjuvant effect (Figure 4).

In contrast, the immunization with OVA–dextrin elicited the production of IgG1 antibodies to levels similar to control animals immunized with OVA alone. Mice treated with nanogels alone did not present OVA-specific IgG1 antibodies. The immunizations did not raise the serum levels of OVA-specific antibodies of the remaining IgG isotypes or of IgA or IgM.

The selective increase in serum IgG1 antibodies indicates that mannan nanogel could favor a T_H2-type immune response, usually associated with antibody production rather than a cellular response as could be inferred from the lack of IgG2a antibodies, associated with a T_H1-type immune response, typically cell mediated.[42,43]

A possible strategy to further boost the humoral response and even to achieve cellular response would consist on the association with other immunostimulants, either entrapped or covalently

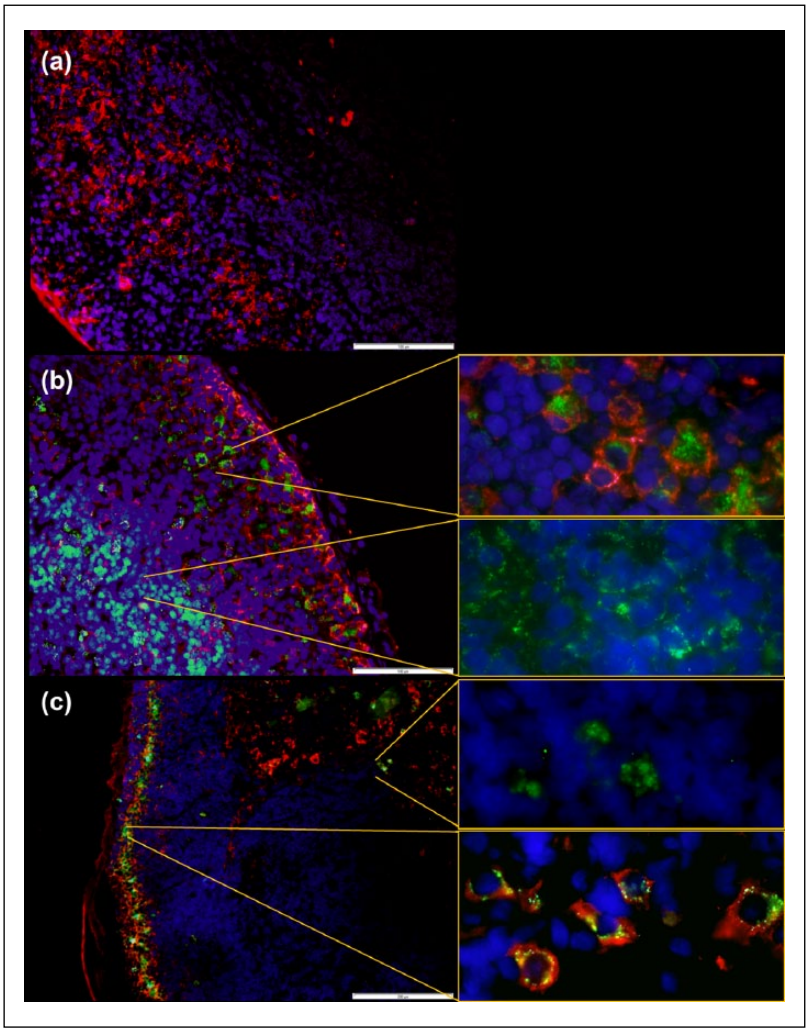

Figure 3. Fluorescence observation of lymph node cryosections stained with anti-CD169 (red) to identify macrophages and with streptavidin dylight 488 to identify biotin-labeled nanogels (green) after footpad injection of nanogels: (a) popliteal node as negative control (without nanogel injection); (b) popliteal node 24 h after footpad injection of mannan nanogels, and (c) popliteal node 24 h after footpad injection of dextrin nanogels,. Nuclei are stained in blue. All images are representative of two independent experiments. Scale bars: 300 µm.

attached to the nanogel. This strategy, that is, a synergistic enhancement of the immune reaction, which may be reached by combining several adjuvant stimuli, has been reported as effective.[44,45] For example, multifunctional chitosan nanoparticles incorporating the recombinant hepatitis B surface antigen and a Toll-like receptor 7 (TLR7) agonist (imiquimod) elicited a specific and predominant T_H1-mediated immune response upon nasal immunization.[46]

The mannose receptor, expressed by a variety of cell types, including dendritic and macrophage cells, is implicated in the recognition and clearance of microorganisms and serum glycoproteins. Although being able to entrap larger amounts of protein and being expected to more effectively

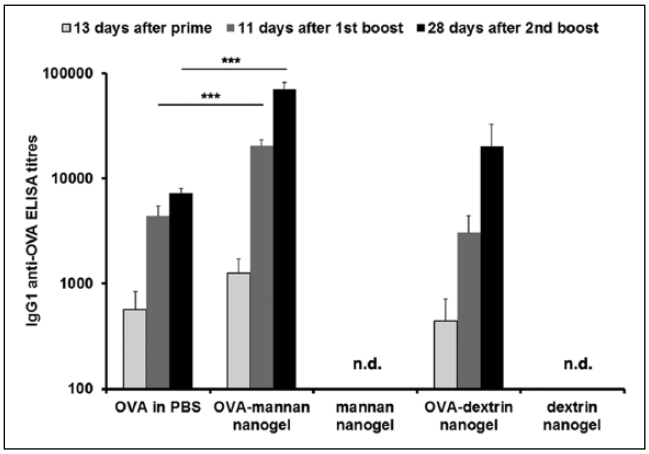

Figure 4. Effect of mannan or dextrin nanogel on serum OVA-specific antibody titers. Groups of male BALB/c mice were trice-immunized (prime, first boost 13 days and second boost 24 days after priming) intradermally with 20 µg OVA formulated with one of the following delivery vehicles (100 µL): mannan nanogel (400 µg) colloidal dispersion in PBS (OVA–mannan nanogel, $n = 5$); dextrin nanogel (400 µg) colloidal dispersion in PBS (OVA–dextrin nanogel, $n = 5$); PBS ($n = 4$). As controls, mannan nanogel ($n = 3$) or dextrin nanogel ($n = 3$) colloidal dispersions in PBS were also injected, completing the five groups in study. The titers are presented as mean ± SD for IgG1 (13 days after priming, 11 days after first boost, and 28 days after second boost) for a representative experiment. Statistical significant differences between respective groups are indicated by horizontal lines (*$p < 0.05$ and ***$p < 0.001$; not detected (n.d.)).

drain to the lymphatic system due the smaller particle size, the dextrin nanogel did not bring any enhancement of the immune reaction, thus mannan seems to play a relevant functional role, as it has been described in the literature.[47,48]

Conclusion

The results showed mannan or dextrin nanogels to be suitable carriers of protein antigens, shown here with OVA as a model antigen. The studied nanogels are not expected to induce major inflammatory responses since they did not induce in vitro activation of the complement cascade.

The mannan nanogel (241 nm) presents higher hydrodynamic diameter than the dextrin nanogel (23 nm), while a similar zeta potential is observed for both nanogels (around −10 mV). After OVA entrapment, size and zeta potential remained almost constant for both formulations. Despite the superior size of mannan nanogel, the entrapment efficient of OVA is lower for this nanogel (36.3%) compared to dextrin nanogel (78.5%). Regarding the nanogels drainage, both are present in the lymph nodes 24 h after administration.

Mannan nanogel, in contrast to dextrin nanogel, showed immunological adjuvant activity on the specific immune response to OVA, predominantly of the humoral type.

The simple methodology, moderate conditions, and that the polymers are medical grade, natural, and biocompatible should all be pointed out as advantages.

Acknowledgements

The authors thank Professor Africa Gonzales for the complement activation analysis at Institute of Biomedical Research (IBIV), Biomedical Research Center (CINBIO), University of Vigo. C.G. and S.A.F. contributed equally to this study.

Declaration of Conflicting Interests

The author(s) declared no potential conflicts of interest with respect to the research, authorship, and/or publication of this article.

Funding

The author(s) disclosed receipt of the following financial support for the research, authorship, and/or publication of this article: This work is supported by the Fundação para a Ciência e a Tecnologia (FCT) Portugal, post-doc grant SFRH/BPD/70524/2010 and the International Iberian Nanotechnology Laboratory (INL), PhD grant. The authors thank the Portuguese Foundation for Science and Technology (FCT) under the scope of the strategic funding of UID/BIO/04469/2013 unit and COMPETE 2020 (POCI-01-0145-FEDER-006684). The authors also acknowledge the Project RECI/BBB-EBI/0179/2012 (FCOMP-01-0124-FEDER-027462).R.

References

1. Lee M, Lee D, Youn Y, et al. Facile fabrication of highly soluble, extremely small-sized drug carriers using globular poly(ethylene glycol). *J Bioact Compat Pol*. Epub ahead of print 17 September 2015. DOI: 10.1177/0883911515603737.
2. Yamane S, Sugawara A, Watanabe A, et al. Hybrid nanoapatite by polysaccharide nanogel-templated mineralization. *J Bioact Compat Pol* 2009; 24: 151–168.
3. Ferreira SA, Gama FM and Vilanova M. Polymeric nanogels as vaccine delivery systems. *Nanomedicine* 2013; 9: 159–173.
4. Raemdonck K, Demeester J and De Smedt S. Advanced nanogel engineering for drug delivery. *Soft Matter* 2009; 5: 707–715.
5. Manning MC, Chou DK, Murphy BM, et al. Stability of protein pharmaceuticals: an update. *Pharm Res* 2010; 27: 544–575.
6. Kambayashi T and Laufer TM. A typical MHC class II-expressing antigen-presenting cells: can anything replace a dendritic cell? *Nat Rev Immunol* 2014; 14: 719–730.
7. Constant SL and Bottomly K. Induction of TH1 and TH2 CD4+ T cell responses: the alternative approaches. *Annu Rev Immunol* 1997; 15: 297–322.
8. Gamvrellis A, Gloster S, Jefferies M, et al. Characterisation of local immune responses induced by a novel nano-particle based carrier-adjuvant in sheep. *Vet Immunol Immunop* 2013; 155: 21–29.
9. Gretz JE, Anderson AO and Shaw S. Cords, channels, corridors and conduits: critical architectural elements facilitating cell interactions in the lymph node cortex. *Immunol Rev* 1997; 156: 11–24.
10. Gerhard W, Mozdzanowska K, Furchner M, et al. Role of the B-cell response in recovery of mice from primary influenza virus infection. *Immunol Rev* 1997; 159: 95–103.
11. Fu K, Klibanov AM and Langer R. Protein stability in controlled-release systems. *Nat Biotechnol* 2000; 18: 24–25.
12. Fu K, Pack DW, Klibanov AM, et al. Visual evidence of acidic environment within degrading poly(lactic-co-glycolic acid) (PLGA) microspheres. *Pharm Res* 2000; 17: 100–106.
13. Tobio M and Alonso MJ. Study of the inactivation process of the tetanus toxoid in contact with poly(lactic glycolic acid) degrading microspheres. *STP Pharma Sci* 1998; 8: 303–310.
14. van der Meel R, Vehmeijer LJC, Kok RJ, et al. Ligand-targeted particulate nanomedicines undergoing clinical evaluation: current status. *Adv Drug Deliver Rev* 2013; 64: 1284–1298.
15. Agarwal R and Roy K. Intracellular delivery of polymeric nanocarriers: a matter of size, shape, charge, elasticity and surface composition. *Ther Deliv* 2013; 4: 705–723.
16. Purwada A, Roy K and Singh A. Engineering vaccines and niches for immune modulation. *Acta Biomater* 2014; 10: 1728–1740.
17. Ferreira SA, Coutinho PJG and Gama FM. Self-assembled nanogel made of mannan: synthesis and characterization. *Langmuir* 2010; 26: 11413–11420.
18. Goncalves C, Martins JA and Gama FM. Self-assembled nanoparticles of dextrin substituted with hexadecanethiol. *Biomacromolecules* 2007; 8: 392–398.
19. Carvalho V, Castanheira P, Faria TQ, et al. Biological activity of heterologous murine interleukin-10 and preliminary studies on the use of a dextrin nanogel as a delivery system. *Int J Pharm* 2010; 400: 234–242.

20. Ferreira SA, Correia A, Madureira P, et al. Unraveling the uptake mechanisms of mannan nanogel in bone-marrow-derived macrophages. *Macromol Biosci* 2012; 12: 1172–1180.
21. Goncalves C, Torrado E, Martins T, et al. Dextrin nanoparticles: studies on the interaction with murine macrophages and blood clearance. *Colloid Surface B* 2010; 75: 483–489.
22. Ferreira SA, Pereira P, Sampaio P, et al. Supramolecular assembled nanogel made of mannan. *J Colloid Interf Sci* 2011; 361: 97–108.
23. Goncalves C, Pereira P, Schellenberg P, et al. Self-assembled dextrin nanogel as curcumin delivery system. *J Biomater Nanobiotechnol* 2012; 3: 178–184.
24. Slutter B, Bal S, Keijzer C, et al. Nasal vaccination with N-trimethyl chitosan and PLGA based nanoparticles: nanoparticle characteristics determine quality and strength of the antibody response in mice against the encapsulated antigen. *Vaccine* 2010; 28: 6282–6291.
25. Wen ZS, Xu YL, Zou XT, et al. Chitosan nanoparticles act as an adjuvant to promote both Th1 and Th2 immune responses induced by ovalbumin in mice. *Mar Drugs* 2011; 9: 1038–1055.
26. Reddy ST, van der Vlies AJ, Simeoni E, et al. Exploiting lymphatic transport and complement activation in nanoparticle vaccines. *Nat Biotechnol* 2007; 25: 1159–1164.
27. Thiele L, Merkle HP and Walter E. Phagocytosis and phagosomal fate of surface-modified microparticles in dendritic cells and macrophages. *Pharm Res* 2003; 20: 221–228.
28. Foged C, Brodin B, Frokjaer S, et al. Particle size and surface charge affect particle uptake by human dendritic cells in an in vitro model. *Int J Pharm* 2005; 298: 315–322.
29. Look M, Bandyopadhyay A, Blum JS, et al. Application of nanotechnologies for improved immune response against infectious diseases in the developing world. *Adv Drug Deliver Rev* 2010; 62: 378–393.
30. Moghimi SM, Andersen AJ, Ahmadvand D, et al. Material properties in complement activation. *Adv Drug Deliver Rev* 2011; 63: 1000–1007.
31. Sjoberg AP, Trouw LA and Blom AM. Complement activation and inhibition: a delicate balance. *Trends Immunol* 2009; 30: 83–90.
32. De Temmerman ML, Rejman J, Demeester J, et al. Particulate vaccines: on the quest for optimal delivery and immune response. *Drug Discov Today* 2011; 16: 569–582.
33. Hawley AE, Davis SS and Illum L. Targeting of colloids to lymph-nodes—influence of lymphatic physiology and colloidal characteristics. *Adv Drug Deliver Rev* 1995; 17: 129–148.
34. Swartz MA. The physiology of the lymphatic system. *Adv Drug Deliver Rev* 2001; 50: 3–20.
35. Reddy ST, Rehor A, Schmoekel HG, et al. In vivo targeting of dendritic cells in lymph nodes with poly(propylene sulfide) nanoparticles. *J Control Release* 2006; 112: 26–34.
36. Manickasingham SP and Sousa CRE. Mature T cell seeks antigen for meaningful relationship in lymph node. *Immunology* 2001; 102: 381–386.
37. Norbury CC. Drinking a lot is good for dendritic cells. *Immunology* 2006; 117: 443–451.
38. Fossum S. The architecture of rat lymph-nodes. 4. Distribution of ferritin and colloidal carbon in the draining lymph-nodes after foot-pad injection. *Scand J Immunol* 1980; 12: 433–441.
39. Carrasco YR and Batista FD. B cells acquire particulate antigen in a macrophage-rich area at the boundary between the follicle and the subcapsular sinus of the lymph node. *Immunity* 2007; 27: 160–171.
40. Junt T, Moseman EA, Iannacone M, et al. Subcapsular sinus macrophages in lymph nodes clear lymph-borne viruses and present them to antiviral B cells. *Nature* 2007; 450: 110–114.
41. Unanue ER, Cerottini JC and Bedford M. Persistence of antigen on surface of macrophages. *Nature* 1969; 222: 1193–1195.
42. Mosmann TR and Sad S. The expanding universe of T-cell subsets: Th1, Th2 and more. *Immunol Today* 1996; 17: 138–146.
43. Stevens TL, Bossie A, Sanders VM, et al. Regulation of antibody isotype secretion by subsets of antigen-specific helper T cells. *Nature* 1988; 334: 255–258.
44. Hamdy S, Elamanchili P, Alshamsan A, et al. Enhanced antigen-specific primary CD4(+) and CD8(+) responses by codelivery of ovalbumin and toll-like receptor ligand monophosphoryl lipid A in poly(D,L-lactic-co-glycolic acid)

nanoparticles. *J Biomed Mater Res A* 2007; 81A: 652–662.
45. Sarti F, Perera G, Hintzen F, et al. In vivo evidence of oral vaccination with PLGA nanoparticles containing the immunostimulant monophosphoryl lipid A. *Biomaterials* 2011; 32: 4052–4057.
46. Vicente S, Peleteiro M, Diaz-Freitas B, et al. Co-delivery of viral proteins and a TLR7 agonist from polysaccharide nanocapsules: a needle-free vaccination strategy. *J Control Release* 2013; 172: 773–781.
47. McKenzie IFC, Apostolopoulos V, Lees C, et al. Oxidised mannan antigen conjugates preferentially stimulate T1 type immune responses. *Vet Immunol Immunop* 1998; 63: 185–190.
48. Tang CK, Lodding J, Minigo G, et al. Mannan-mediated gene delivery for cancer immunotherapy. *Immunology* 2007; 120: 325–335.